

by the angle which it makes with them. At low temperatures the effect of long-wavelength magnons will be to cause motions in which the impurity and

its neighbors move substantially as a unit preserving their mutual orientation. An improved theory would take this effect into account.^{18,19}

*Supported in part by the National Science Foundation.

†Supported in part by the U. S. Office of Naval Research and the National Science Foundation.

¹S. W. Lovesey, *J. Phys. C* **1**, 102 (1968); T. Tonegawa, *Progr. Theoret. Phys. (Kyoto)* **40**, 1195 (1968); E. Shiles and D. Hone, *J. Phys. Soc. Japan* **28**, 51 (1970).

²T. Wolfram and J. Callaway, *Phys. Rev.* **130**, 2207 (1963); T. Wolfram and W. Hall, *ibid.* **143**, 284 (1966).

³D. Hone, H. B. Callen, and L. R. Walker, *Phys. Rev.* **144**, 283 (1966).

⁴M. Butler, V. Jaccarino, N. Kaplan, and H. J. Guggenheim, *Phys. Rev.* **B1**, 3058 (1970); see also E. Shiles and D. Hone, Ref. 1.

⁵H. B. Callen, *Phys. Rev.* **130**, 890 (1963).

⁶H. B. Callen and S. Shtrikman, *Solid State Commun.* **3**, 5 (1965).

⁷L. R. Walker, B. B. Cetlin, and D. Hone, *J. Phys. Chem. Solids* **30**, 923 (1969).

⁸T. Tonegawa and J. Kanamori, *Phys. Letters* **21**, 130 (1966).

^{8a}V. Jaccarino (unpublished).

⁹O. Nikotin, P. A. Lindgard, and O. W. Dietrich, *J. Phys. C* **2**, 1168 (1969).

¹⁰F. M. Johnson and A. M. Nethercot, *Phys. Rev.* **104**, 847 (1956); **114**, 705 (1959).

¹¹L. F. Johnson, R. E. Dietz, and H. J. Guggenheim, *Phys. Rev. Letters* **17**, 13 (1966).

¹²R. Weber, *Phys. Rev. Letters* **21**, 1260 (1968).

¹³G. K. Wertheim, H. J. Guggenheim, and D. N. E. Buchanan, *J. Appl. Phys.* **40**, 1319 (1969).

¹⁴M. E. Lines, *Phys. Rev.* **156**, 543 (1967).

¹⁵T. M. Holden, W. J. L. Buyers, and R. W. H. Stevenson, *J. Appl. Phys.* **40**, 991 (1969).

¹⁶F. J. Dyson, *Phys. Rev.* **102**, 1217 (1955); **102**, 1230 (1955).

¹⁷F. Keffer and R. Loudon, *J. Appl. Phys.* **32**, 25 (1961).

¹⁸D. Hone, D. J. Scalapino, and R. Silbergliitt, *J. Appl. Phys.* **41**, 948 (1970).

¹⁹S. Watarai and T. Kawasaki (unpublished).

Electrical Resistivity and the Depression of the Néel Temperature in Cr-Mo and Cr-Fe

M. A. Mitchell and J. F. Goff

Naval Ordnance Laboratory, White Oak, Silver Spring, Maryland 20910

(Received 30 August 1971)

Existing data are used to show that Mo and Fe impurities cause the Néel temperature T_N of Cr to decrease at almost exactly the same rate up to 10 at.%. Elements with a higher valence than Cr generally increase T_N . It is suggested that two Fe electrons are localized and produce a localized magnetic moment, for which experimental evidence already exists. The effective valence of Fe would then be similar to that of Mo. In order to investigate the similarities and differences of Cr-Fe and Cr-Mo, electrical-resistivity measurements have been made on two Cr alloys with 9.35-at.% Mo and 9.35-at.% Fe, respectively, from 2 to 300°K. For Cr-Mo, $T_N=197^\circ\text{K}$, and for Cr-Fe, $T_N=181^\circ\text{K}$. At 0 and 200°K the resistivity of Cr-Fe is 12.6 and 3.2 times higher, respectively, than that of Cr-Mo. We suggest that localized magnetic moments at Fe sites combined with atomic disorder produce a large, nearly temperature-independent spin-disorder scattering in Cr-Fe. A simple model of electrical conduction is employed to explain the temperature dependence of the electrical resistivity. Below T_N an energy gap with a BCS temperature dependence opens up over a part of the Fermi surface, and conduction takes place in two bands. As a result of the gap, electrons in the magnetic band are thermally frozen out with decreasing temperature, which leads to the rise in resistivity just below T_N . The 0°K gap is estimated to be 0.14 eV for Cr-Mo and 0.072 eV for Cr-Fe. Pure Cr and Cr-Mo have nearly the same balance of conduction between the magnetic and nonmagnetic bands. In Cr-Fe the balance is shifted toward conduction in the magnetic band.

I. INTRODUCTION

The purpose of this paper is twofold. First we would like to point out that Mo and Fe impurities lower the Néel temperature T_N of chromium at almost exactly the same rate up to concentrations of the order of 10 at.%. This likeness does not

seem to have been noted before, although Suzuki has commented that there is an order-of-magnitude similarity.¹ Iron is anomalous since most other elements of higher valence than Cr cause T_N to increase.

Second, we report an analysis of the electrical resistivity of two Cr alloys containing 9.35 at.%

Mo and Fe, respectively, which have been measured in the temperature range 2–300 °K in order to investigate the similarities and differences of the two cases. The method of analysis is similar to that used previously² but is simplified in that some of the details of the distribution of electrons about the Fermi surface are neglected. It will be seen from this analysis that, although the T_N 's of the two samples are nearly the same, there are differences between the antiferromagnetic energy gaps and between the ratio of conduction on the antiferromagnetic and paramagnetic Fermi surfaces. Furthermore, an additional scattering process in Cr-Fe accounts for its high electrical resistivity relative to Cr-Mo. This process is thought to be magnetic in origin.

The remainder of this paper is divided into the following four parts: The sample characteristics and experimental details are given in Sec. II; in Sec. III, the depression of T_N is discussed; the resistivity of the Cr-Mo and Cr-Fe specimens which we have measured is presented and analyzed in Sec. IV; Sec. V is a summary.

II. EXPERIMENTAL DETAILS

Pure iochrome (99.996%) was obtained from the Materials Research Corporation (Orangeburg, New York); pure molybdenum (99.985%) was obtained from Jarrell-Ash (Waltham, Mass.); and pure iron (99.999%) from United Mineral and Chemical Corporation. The basic constituents of each of the two alloys were arc melted together and remelted 2–3 times in the form of a button; this was finally remelted into the form of a crude bar. The Cr-Mo bar was annealed at 800 °C for 2 h and then ground to the shape of a square rod about 4×4×65 mm. The nominal concentration of Mo was 8.96 at.%. A wet chemical analysis of an end piece indicated that the sample contained 9.35 at.% Mo. The latter is considered to be more accurate because the much higher melting temperature of the Mo could result in the evaporation of a disproportionate amount of Cr during melting.

The crude Cr-Fe bar was annealed at 900 °C for 24 h and then ground to the shape of a square rod 4×4×59 mm. Radiographic x-ray examination showed the presence of three small, spherical inclusions (0.03 cm in diameter) of greater x-ray density than the rest of the matrix, and near the center of the rod. It was estimated that such inclusions had much less than 1% effect on the transport properties.

The Cr-Fe sample was reannealed for 24 h at 900 °C followed by an air quench. Its nominal composition was 9.35 at.%.

Electrical resistivity was measured by the four-probe method. A very stable electronic constant-voltage supply provided current, and voltages were

measured between two voltage probes which also served as thermometer mounts using a Leeds and Northrup K-3 potentiometer. Carbon thermometers were used below 77 °K and platinum thermometers above.

Random scatter about a smooth curve through the resistivity data was less than 1%. The largest systematic error, in the geometry factor, was 1–2%, and this determined the absolute error, 1–2%.

III. LOWERING OF T_N

A. General Effect of Alloying

It has been experimentally established that at its Néel temperature (313 °K) pure chromium undergoes a first-order phase transition from the paramagnetic state to a unique kind of antiferromagnetic state.^{3,4} Between 313 and 121 °K a conduction-electron spin-density wave (SDW) is formed whose wave vector \vec{Q} is incommensurate with the reciprocal lattice, i. e., $\vec{Q} = (\pi/d)(1 \pm \delta, 0, 0)$ where $\delta \approx 0.06$ and d is the lattice spacing; the spin polarization is transverse. Below the spin-flip temperature (121 °K) the spin polarization is longitudinal.

When other transition metals are alloyed with chromium there are changes in the antiferromagnetic state.^{1,5–8} In general, elements which have a smaller valence than Cr lower T_N and the average magnetic moment per atom ($\langle \mu \rangle$) and increase δ . The elements molybdenum and tungsten also do this. Most of the elements with a higher valence initially increase T_N and $\langle \mu \rangle$ and decrease δ . Iron, cobalt, and nickel are anomalous—they lower T_N . When $\delta \rightarrow 0$ a new, stable, commensurate antiferromagnetic state is formed. In many cases a mixture of commensurate and transverse incommensurate states exists in certain concentration ranges (e. g., in Cr-Mn⁹ and Cr-Fe⁶). Longitudinally polarized SDW's are not found above 2 at.%.

On the theoretical side, the band structure proposed by Lomer¹⁰ describes the qualitative features of the Fermi surface. There is a large, octahedrally shaped pocket of electrons at the center of the Brillouin zone and large, octahedral hole pockets on the [100] axes at the edges of the Brillouin zone; there are six smaller, closed electron surfaces between the electron and hole octahedra. Another set of hole pockets described by Lomer was not found in the band calculations of Loucks.¹¹ The antiferromagnetism of chromium arises from an exchange-induced pairing of electrons on the surface of the electron octahedron with holes in parallel sheets of the hole surface. The surfaces are separated by the vector \vec{Q} . The electron octahedron is slightly smaller than the hole octahedron, and the magnitude of \vec{Q} is slightly different from $\frac{1}{2}$ reciprocal-lattice vector.

On the basis of this band model it may be seen

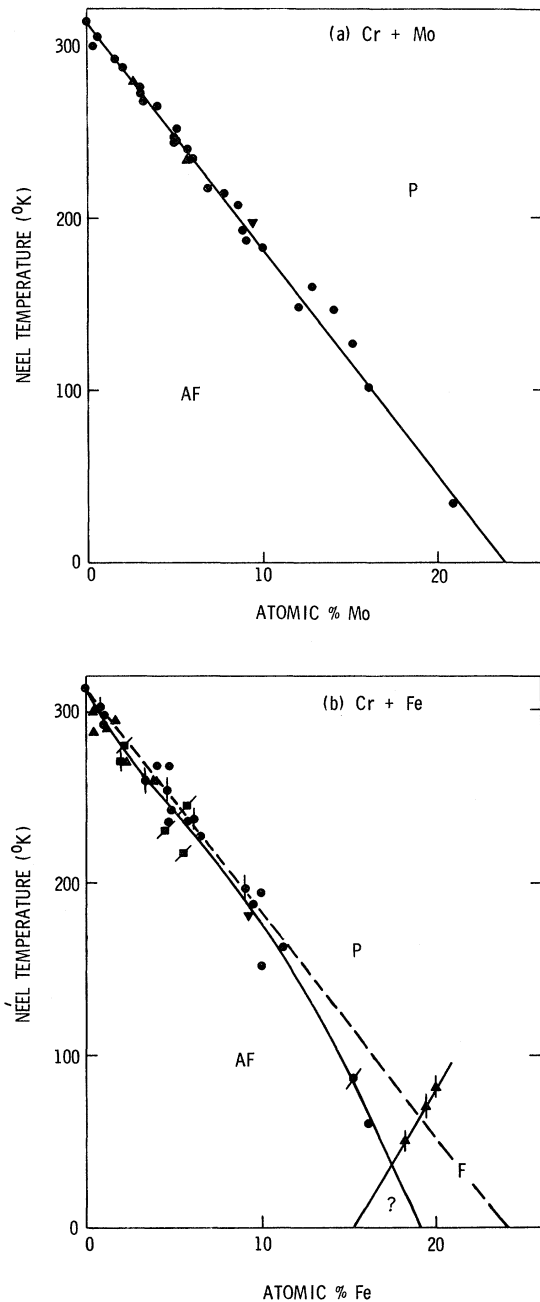


FIG. 1. Depression of the Néel temperature of Cr by Mo and Fe. Data in (a) and (b) were obtained from electrical resistivity, circle; integrated neutron intensity, triangle; magnetic susceptibility, circle with vertical slash; thermal expansion, square with diagonal slash; paramagnetic resonance, square with vertical slash; electrical resistivity, Ref. 25, circle with diagonal slash; and electrical resistivity, this work, inverted triangle. AF, P, and F refer to the antiferromagnetic, paramagnetic, and ferromagnetic states, respectively. Ferromagnetic Curie temperatures are also plotted in (b), triangle with vertical slash. Dashed line is the same as solid line in (a). Note the region of overlap of AF and F from 15.4 to 19.0 at. % Fe.

that valence can play a primary role in changing T_N , $\langle \mu \rangle$, and \bar{Q} . If the band structure does not change much, alloying chromium with higher valence elements should cause the electron octahedron to increase and the hole octahedron to decrease, resulting in a more complete matching of the two surfaces. The stability of the antiferromagnetic state is thereby improved; T_N and $\langle \mu \rangle$ increase, and δ decreases. The converse is true for lower valence elements. This picture seems to explain well the behavior of Cr-V and Cr-Mn alloys. Putting vanadium (valence 5) into chromium (valence 6) lowers T_N , and manganese (valence 7) raises T_N .⁹ When T_N is plotted against electron number, the T_N curve for the ternary alloy Cr-V-Mn falls on top of the T_N curves for the binary alloys.¹²

B. Reduction of T_N by Mo and Fe

In Figs. 1(a) and 1(b), the transition temperatures for Cr-Mo and Cr-Fe, respectively, are plotted. The antiferromagnetic transition produces well-defined anomalies in several properties of Cr and its alloys, and these may be used to find T_N . For Cr-Mo [Fig. 1(a)] integrated neutron intensity⁵ and electrical resistivity^{1,8,13-19} were used. For Cr-Fe [Fig. 1(b)] integrated neutron intensity,^{6,20,21} electrical resistivity,^{8,22-27} magnetic susceptibility,^{28,29} and thermal expansion^{1,6,22,30} were used. The dashed line in Fig. 1(b) is the same as the solid line in Fig. 1(a). The effect of Fe on T_N is strikingly similar to that of Mo below 10 at. %, but above this percentage, Fe reduces T_N more rapidly than Mo.

The depression of the T_N by isoelectronic Mo is more subtle than the valence effect of V and Mn. Koehler *et al.*⁵ have suggested an explanation in the context of the Fedders and Martin theory.³¹ The latter derived

$$T_N = T_B e^{-1/\lambda}, \quad (1)$$

$$\lambda = \gamma^2 V(0) k_c^2 / 2\pi^2 v_F,$$

where T_B is a constant which depends on the band structure; k_c is the average radius of the Fermi surface (the electron and hole surfaces are spherical and congruent in this model); v_F is the average Fermi velocity; $V(0)$ is the average screened-Coulomb potential; and γ is a mean overlap matrix element for intraband electrons. The addition of Mo affects the Fermi surface less than elements with a different valence; this is supported by the experimental result that δ varies much less rapidly with the addition of Mo than other elements.⁵ However, the $4d$ wave functions of Mo are less localized than the $3d$ wave functions of Cr,³² and therefore, the overlap factor, γ , is reduced. Then λ in Eq. (1) is also reduced, and T_N decreases.

Whether or not this particular explanation is correct, it is reasonable to expect some effect of the $4d$ nature of Mo on T_N .

There is experimental evidence for the existence of localized magnetic moments on Fe impurities in Cr-Fe alloys^{1, 6, 7}; above T_N this magnetic moment is about $2\mu_B$ ($\mu_B = 1$ Bohr magneton).⁶ Neutron-diffraction measurements on a piece of the Cr-Fe specimen reported here³³ indicated that the alloy was commensurate down to 4.2°K , which is consistent with a locking of SDW's to the lattice by localized magnetic moments.³⁴ Furthermore, a large scattering of electrons by magnetic Fe impurities would give rise to the high electrical resistivity of Cr-Fe relative to Cr-Mo, to be discussed in Sec. IV. A localization of two electrons at Fe sites would explain the localized magnetic moment. Since the effective valence of Fe would then be the same as Mo, localization would also help explain why the two elements decrease T_N at the same rate.

Barker *et al.*³⁵ have pointed out that scattering can have a pair-breaking effect on electron-hole pairs in Cr, and thereby cause a reduction in T_N . By means of the formalism of Zittartz³⁶ they calculated that the Néel temperature of pure Cr unrenormalized by electron-phonon scattering is 750°K . Impurity scattering may explain, at least in part, the reduction of T_N in Cr-Mo.¹⁹ In Cr-Fe, all other considerations aside, if the valence effect were overcompensated by the large extra scattering (see Sec. IV), T_N would fall with the addition of Fe as is observed; but in Cr-Mn,^{37, 38} in which the electrical resistivity is as large as in Cr-Fe, T_N is observed to increase with increasing Mn concentration. Thus, the quantitative importance of the effect of scattering on T_N is not clear.

The onset of ferromagnetism occurs at or near the concentration at which antiferromagnetism disappears in Cr-Fe, as Baum and Schroeder³⁹ have so recently pointed out. In fact, the extrapolation of the ferromagnetic Curie temperature data⁴⁰ to zero in Fig. 1(b) indicates that from 15.4 to 19.0 at. % Fe the ferromagnetic and antiferromagnetic states overlap. It is interesting to note that the peak in the electronic specific-heat coefficient of Cr-Fe occurs at 19 at. % Fe.⁴¹ The peak in the electronic specific-heat coefficient of Cr-Mo occurs at 24 at. % Mo,¹⁴ where antiferromagnetism is known to disappear.⁴² The region of overlap in Cr-Fe would be worthy of more experimental investigation.

IV. ELECTRICAL RESISTIVITY OF Cr-Mo AND Cr-Fe

The electrical resistivity of the two specimens, Cr + 9.35 at. % Mo and 9.35 at. % Fe, is plotted in Fig. 2. The resistivity of Cr-Mo agrees well with

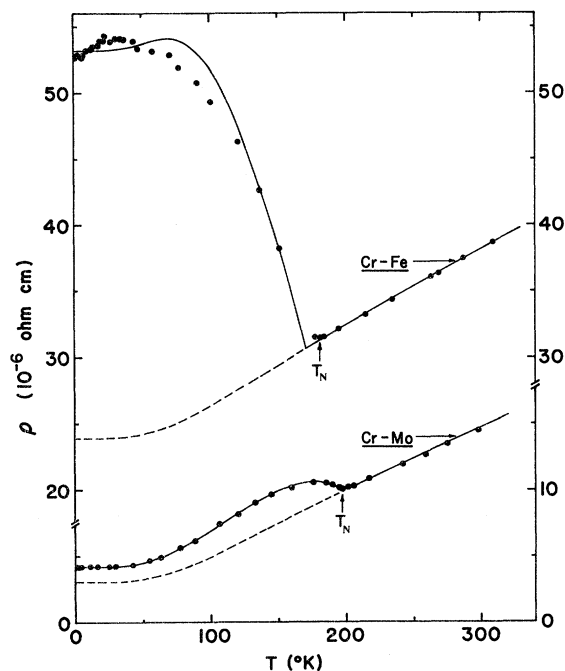


FIG. 2. Electrical resistivity of Cr 9.35 at. % Mo (lower data) and Cr 9.35 at. % Fe (upper data). Solid line through each set of data points was calculated from resistivity model. Dashed lines are extrapolations of the paramagnetic state according to the resistivity model. For Cr-Mo, $T_N = 197^\circ\text{K}$, and for Cr-Fe, $T_N = 181^\circ\text{K}$.

Arajs's measurement of an 8.8-at. % Mo alloy.¹³ The Cr-Fe resistivity in Fig. 2 is similar to that of a 9.5-at. % Fe specimen reported by Arajs and Dunmyre.²⁶ Below 30°K the data have a slight temperature dependence which is stronger than one would expect from lattice scattering. Although this temperature dependence is not understood, it is nearly $T^{3/2}$, and magnetic scattering is suspected.

Above T_N the resistivity of both alloys is nearly linear, but the data are slightly concave upwards. A similar concavity is observed in pure Cr above T_N .⁴³

The rise of resistivity below the Néel temperature in Fig. 2 is in both cases due to the effect of the opening of an energy gap over part of the Fermi surface, but the resistivity of Cr-Fe is much larger than that of Cr-Mo over this temperature range. It is believed here that there is a large magnetic scattering in addition to the impurity scattering, since nonmagnetic properties such as valence generally do not produce this large an effect.⁴⁴ The addition of Mo to Cr reduces the average magnetic moment per atom below T_N .⁵ On the other hand, the magnetic moment per atom is significantly increased with the addition of Fe, and a localized moment of about $2\mu_B$ has been associated with the

Fe impurities.²⁹

In certain respects Cr-Fe is analogous to gadolinium (and other rare earths). In the case of Gd above its Curie temperature,⁴⁵ the atomic spins are thermally disordered, and a large, temperature-independent resistivity ρ_m in addition to the lattice resistivity is observed. Below the Curie temperature the Gd spins order magnetically, and the resistivity becomes more temperature dependent; it falls to zero at absolute zero. Now assume that Fe impurities in Cr have atomic spins, and that they are spatially disordered. This situation is analogous to Gd above its Curie temperature—except that the spatial disorder remains in Cr-Fe below T_N , and consequently the large resistivity remains almost temperature independent below T_N . This assumption will be used presently.

Klemen's formulation of transport coefficients⁴⁶ has been used by Goff² to explain the temperature dependence and magnitude of the Lorenz number, thermal conductivity, and electrical resistivity of pure Cr. Band structure was incorporated into the analysis and was found to have an important influence on the transport properties. This treatment will now be adapted to the alloys, although the band-structure effects will be neglected in order to simplify the problem.

The electrical conductivity is²

$$\sigma(T) = - \int_{-\infty}^{\infty} \sigma(E) \frac{\partial f_0}{\partial E} dE, \quad (2)$$

where E is the electron energy measured from the Fermi level; $f_0 = [\exp(E/k_B T) + 1]^{-1}$; k_B and T are the Boltzmann constant and absolute temperature, respectively; and $\sigma(E)$ is the energy-dependent conductivity⁴⁶

$$\sigma(E) = \frac{e^2}{4\pi^3} \int_S \frac{\tau v_x^2 dS}{|\text{grad}_{\vec{k}} E|}. \quad (3)$$

Here τ is the relaxation time, v_x is the velocity in the direction of current, \vec{k} is the electron wave vector, S is a constant energy surface in \vec{k} space, and e is the electronic charge. In the case of a degenerate, free-electron gas

$$\sigma(T) \approx \frac{1}{3} N(0) e^2 v_F^2 \tau, \quad (4)$$

where $N(0)$ is the electron density of states at the Fermi level.

In Cr and its antiferromagnetic alloys an energy gap opens up over part of the Fermi surface, and a portion of the current carriers in the metal are frozen out of the conduction process. The electrical conductivity of these metals therefore looks similar to a two-band situation in which one band has metallic conductivity which decreases with increasing temperature, and the other band has a semiconducting conductivity which increases with

increasing temperature. In order to treat the above case assume that τ is isotropic; take $v_x^2 = \frac{1}{3} v^2(E)$; and remove the $\tau v^2(E)$ product from within the surface integral in Eq. (3). The integral that is left is the density of states. Now divide the surface S into a normal part S_p and a magnetic part S_A .

Equation (3) becomes

$$\sigma(E) = \sigma_p(E) + \sigma_A(E), \quad (5)$$

where the p and A subscripts refer to the nonmagnetic and magnetic parts of S , respectively; and we have defined

$$\sigma_p(E) = \frac{1}{3} e^2 v^2(E) \tau(E) N_p(E), \quad (6)$$

$$\sigma_A(E) = \frac{1}{3} e^2 v^2(E) \tau(E) N_A(E). \quad (7)$$

Fedders and Martin³¹ derived a BCS⁴⁷ density of states and energy gap in their model. With some changes this result will be used here. For $T \leq T_N$,

$$\frac{\sigma_A(E)}{\sigma_p(E)} = \begin{cases} \frac{R|E|}{(E^2 + \Delta^2)^{1/2} + \xi \cdot k_B T}, & E > \Delta \\ 0, & E \geq \Delta \end{cases} \quad (8)$$

and $\sigma_A(E)/\sigma_p(0) = R$ for $T > T_N$. The ratio R is given by

$$R = \frac{\tau(E) v^2(E) N_A(0)}{\tau(0) v^2(0) N_p(0)}, \quad (9)$$

where $N_A(E)$ is the density of states which would exist at the magnetic surface S_A if there were no antiferromagnetic transition, i. e., $\Delta = 0$. The constant ξ is taken to be small, and Δ is an energy gap with the temperature dependence of the BCS gap $[\Delta(T)/\Delta(0)]$ is tabulated in Ref. 48]. Using Eqs. (2), (5), (7), and (8),

$$\sigma(T) = \sigma_p(0) \left(- \int_{-\infty}^{\infty} \frac{\sigma_p(E)}{\sigma_p(0)} \frac{\partial f_0}{\partial E} dE + R I_A \right), \quad (10)$$

where

$$I_A = 2 \int_{\Delta_R}^{\infty} \frac{z}{(z^2 - \Delta_R^2)^{1/2} + \xi} \frac{e^z}{(e^z + 1)^2} dz \quad (11)$$

and

$$\Delta_R = \frac{\Delta(T)}{k_B T} = \Delta_0 \frac{T_N}{T} \frac{\Delta(T)}{\Delta(0)}. \quad (12)$$

The integral I_A must be evaluated as a function of its lower limit Δ_R . In the BCS theory,⁴⁷ $\Delta_0 = 1.75$, but we treat it as a parameter. Suppose that $\sigma_p(E)/\sigma_p(0)$ is slowly varying for Cr-Fe and Cr-Mo in the range $-4k_B T < E < 4k_B T$. In this case

$$- \int_{-\infty}^{\infty} \frac{\sigma_p(E)}{\sigma_p(0)} \frac{\partial f_0}{\partial E} dE \approx 1. \quad (13)$$

After substituting Eq. (13) into Eq. (10), the re-

sistivity is

$$\rho(T) = \frac{1}{\sigma(T)} = \frac{1}{\sigma_p(0)} \frac{1}{1 + RI_A}. \quad (14)$$

In order to apply Eq. (14) to Cr-Mo it is assumed that

$$\frac{1}{\sigma_p(0)} = \rho_0 + \rho_i(T). \quad (15)$$

The resistivity ρ_0 is temperature independent, and $\rho_i(T)$ the lattice resistivity. The latter is taken to have the temperature dependence of the Bloch-Grüneisen law⁴⁹

$$\rho_i(T) = a(T/\Theta_R)^5 J_5(\Theta_R/T), \quad (16)$$

where a and Θ_R are a constant and electrical Debye temperature, respectively; and $J_5(\Theta_R/T)$ is a function which is tabulated in Ref. 49.

The constants R , Δ_0 , a , and Θ_R were adjusted to fit Eq. (14) to the electrical-resistivity data of Cr-Mo from 2–300 °K. This fit is the solid line through the Cr-Mo data in Fig. 2, and the values of the constants are listed in Table I. The Debye temperature from specific-heat measurements Θ_D is also listed for comparison. The Θ_R is less than Θ_D , but this is found to be true for other metals also.⁴⁴ The fit is very good for Cr-Mo.

The Cr-Fe resistivity is more complicated. We assume that the magnetic resistivity ρ_m and the normal impurity resistivity are lumped into ρ_0 in Eq. (15). The Θ_R for Cr-Fe is assumed to be the same as for Cr-Mo because in this case the fit is insensitive to the choice of Θ_R . Just below $T_N = 181$ °K (the minimum in resistivity), from 171 to 181 °K, the rise of resistivity is relatively slow, and there seems to be a precursor. This was ignored by taking $T_N = 171$ °K for the purposes of the resistivity analysis. The values of the constants R , a , Δ_0 , and Θ_R for Cr-Fe in Table I produced the solid-curve fit of Eq. (14) to the Cr-Fe resistivity data in Fig. 2. Although the model does not work as well in this case as for Cr-Mo, it does serve to explain the main features of the resistivity and to estimate the antiferromagnetic energy gap

and R .

The pure-Cr data of Goff² have been reanalyzed using a BCS-gap temperature dependence. Previously,² the gap was assumed to be proportional to $(1 - T/T_N)^{1/2}$, which is BCS-like only near T_N . The new constants R and Δ_0 thus obtained are included in Table I.

There are several important approximations in this resistivity model: (i) An isotropic relaxation time is assumed. (ii) It is assumed that $\sigma_p(E)$ is well behaved and slowly varying so that Eq. (13) is true. In pure Cr it is not, and at 200 °K Eq. (13) is only 90% correct. The Lorenz number L can indicate whether $\sigma_p(E)$ is well behaved by the amount by which it differs from the Sommerfeld value. In Cr-Mo, L is smaller than in Cr, and it is perhaps 15% higher at most than the Sommerfeld value.⁵⁰ Thus, the approximation of Eq. (13) is probably fairly good. On the other hand, Cr-Fe has a large, strangely behaved Lorenz number (we have measured it), and the approximation is not as good. (iii) The use of a BCS density of states and gap temperature dependence may be an oversimplification. (iv) The Bloch-Grüneisen law has never worked well in transition metals and alloys. (v) The magnetic part of the electrical resistivity of Cr-Fe may have a temperature dependence caused by magnetic ordering.

The ratio R of A -surface to p -surface electrical conductivity is proportional to (but not simply equal to) the ratio of the density of states $N_A(0)/N_p(0)$, as can be seen from Eq. (9). In this analysis R is supposed to be constant; this will be true only if the ratio $\tau(E)v^2(E)/\tau(0)v^2(0)$ is temperature and energy independent. Other authors deal with the ratio $\alpha = N_p(0)/[N_p(0) + N_A(0)]$. If $\tau(E)v^2(E)/\tau(0)v^2(0) \approx 1$ in Eq. (9), then R and α are simply related: $\alpha \approx R/(R+1)$. We have included $R/(R+1)$ in Table I.

A comparison of the conductivity of Cr and the Cr-Mo and Cr-Fe alloys is made in Table II. The X and Y superscripts refer to Cr or one of the two alloys listed in column 1. The conductivity of Cr-Mo is more than an order of magnitude higher than Cr-Fe at 0 °K (column 2), and more than 3 times

TABLE I. Parameters of the electrical-resistivity model.

Sample	T_N (°K)	R	$\frac{R}{R+1}$	Δ_0	$2\Delta_0 k_B T_N$ (eV)	ρ_0^a ($\mu\Omega$ cm)	a ($\mu\Omega$ cm)	Θ_R (°K)	Θ_D (°K)
Pure Cr	313	0.464	0.32	1.89	0.102	575 ^b
Cr 9.35 at. % Mo	197	0.395	0.28	3.64	0.124	4.19	98.14	405	550 ^c
Cr 9.35 at. % Fe	181 ^d	1.219	0.55	2.45	0.072	53.2	187.4	405	235 ^e

^aNote that above T_N the total resistivity is $[\rho_0 + \rho_i(T)]/(R+1)$. This also gives the paramagnetic resistivity below T_N .

^bComposite value: J. F. Goff, Phys. Rev. B 4, 1121 (1971).

^cReference 14.

^d $T_N = 171$ °K was used in fitting the model to the Cr-Fe resistivity data.

^eReference 41.

TABLE II. Comparison of electrical conductivity.

(1)	(2)	(3)	(4)	(5)
X/Y	$\frac{\sigma_p^X(0)}{\sigma_p^Y(0)} \Big _{T=0^\circ\text{K}}$	$\frac{\sigma^X(200^\circ\text{K})}{\sigma^Y(200^\circ\text{K})}$	$\frac{\sigma_p^X(0)}{\sigma_p^Y(0)} \Big _{T=200^\circ\text{K}}$	$\frac{\sigma_A^X(0)}{\sigma_A^Y(0)} \Big _{T=200^\circ\text{K}}$
Cr/Cr-Mo	...	1.28	1.6	1.9
Cr/Cr-Fe	...	4.1	8.3	3.2
Cr-Mo/Cr-Fe	12.6	3.2	5.2	1.7

higher at 200 °K (column 3). At 200 °K the conductivity of Cr is only 28% higher than Cr-Mo, but 410% higher than that of Cr-Fe as a result of the magnetic scattering in the latter. Columns 4 and 5 show that in going from pure Cr to Cr-Mo there is not much change in the balance of conduction by the magnetic and nonmagnetic surfaces (compare 1.6 to 1.9), but that there is a shift toward more conduction on the magnetic surface in going from Cr to Cr-Fe (compare 8.3 to 3.2); that R is higher for Cr-Fe than for Cr-Mo or Cr also supports this conclusion.

It can be seen in Table I that the energy gap for Cr-Mo is larger than that of Cr-Fe. Barker and Ditzemberger⁸ found the converse to be true in an optical-absorption study: For Cr + 8.6 at. % Mo, $\Delta_0 = 2.55$ ($2\Delta_0 k_B T_N = 0.091$ eV) and $\alpha = 0.33$, while for Cr-Fe the 0 °K gap was 0.23 eV. They also found that for pure Cr, $\Delta_0 = 2.55$ ($2\Delta_0 k_B T_N = 0.14$ eV). McWhan and Rice⁵¹ obtained $\Delta_0 = 2.3$ ($2\Delta_0 k_B T_N = 0.13$ eV) and $\alpha = 0.3$ in their study of the effect of hydrostatic pressure on the electrical resistivity of pure Cr. Heiniger¹⁴ measured the specific heat of Cr and Cr alloys at low temperatures and obtained the electronic specific-heat coefficient for the paramagnetic γ_p and antiferromagnetic γ_A states. These are simply related to α : $\alpha = 1 - \gamma_A/\gamma_p$. Using Heiniger's data, $\alpha = 0.52$ in pure Cr and 0.37 in Cr + 9 at. % Mo [compare with $R/(R+1)$ in Table I]. Considering the diversity of methods used in obtaining these data, over-all agreement should be considered very good.

V. SUMMARY

We have used existing data to show that Mo and Fe impurities depress the Néel temperature of Cr at almost exactly the same rate up to 10 at. % (see Fig. 1). That Fe impurities lower T_N is unexpected since most elements with a greater valence than Cr initially raise T_N . There is experimental evidence for the existence of localized magnetic moments at Fe sites.^{1, 6, 7} Two localized Fe electrons could give rise to both localized moments and a lower effective Fe valence, which in turn would partially explain the observed effect of Fe on T_N . However, the band structure of antiferromagnetic Cr alloys has not been calculated in detail, and the effects of scattering of electrons³⁵ and the $4d$ nature of Mo⁵ on T_N

are poorly understood. Consequently, it is not possible to draw definite conclusions about the similarity of the effect of Mo and Fe on T_N .

Electrical-resistivity measurements of two alloys, Cr + 9.35 at. % Mo and Fe, respectively, between 2 and 300 °K have been reported here. It is possible to explain the temperature dependence of the resistivity of Cr-Mo by means of a simple model with four adjustable parameters. The model has the following features. Above T_N conduction is limited by impurity scattering and lattice scattering which can be calculated from the Bloch-Grüneisen law with a Debye temperature of 405 °K. At the magnetic transition an energy gap with a BCS temperature dependence^{47, 48} opens up over part of the Fermi surface, and there is conduction in the equivalent of two bands. The thermal freezing out of current carriers in the magnetic band as a result of the gap leads to the rise of resistivity just below T_N , and eventually conduction takes place only in the nonmagnetic band. The 0 °K energy gap (an adjustable parameter) is 0.12 eV. The model fits the resistivity of Cr-Mo very well in the temperature range 2–300 °K.

The Cr-Fe alloy is more complicated. For one thing its resistivity is considerably larger than that of Cr-Mo. We suggest that a combination of localized magnetic moments on Fe sites and atomic disorder produces a large spin-disorder resistivity which is fairly temperature independent, even below T_N . This magnetic contribution is lumped in with the impurity resistivity. The resistivity model was fit to the Cr-Fe data from 2 to 300 °K since the data below 35 °K were anomalous. The 0 °K energy gap was 0.072 eV. Although the model does not fit Cr-Fe as well as Cr-Mo, the important features of the resistivity are reproduced, and rough estimates of the parameters can be made.

The balance of electrical conduction between the magnetic and nonmagnetic parts of the Fermi surface is almost the same in Cr-Mo as in pure Cr. However, in Cr-Fe the balance is shifted toward conduction on the magnetic surface, with consequent enhancement of ρ below T_N .

Previous experimental estimates of the energy gap in pure Cr are 0.13 eV⁵¹ and 0.14 eV,⁸ and in Cr 8.6 at. % Mo, 0.091 eV.⁸ Commensurate alloys (e.g., Cr-Fe) were found to have a larger gap than

incommensurate ones (e. g., Cr-Mo),⁸ but we find the converse. Nevertheless, over-all agreement between ours and previous data is good.

ACKNOWLEDGMENTS

The authors wish to thank J. J. Rhyne, J. R.

Cullen, and W. Buehler for informative and helpful conversations, and S. Pickart for making neutron-diffraction measurements on the Cr-Fe alloy. We appreciate the help of R. Jones in sample preparation.

- ¹T. Suzuki, *J. Phys. Soc. Japan* **21**, 442 (1966).
²J. F. Goff, *Phys. Rev. B* **1**, 1351 (1970); **2**, 3606 (1970).
³L. M. Corliss, J. M. Hastings, and R. J. Weiss, *Phys. Rev. Letters* **3**, 211 (1959).
⁴A. Arrott, A. Werner, and H. Kendrick, *Phys. Rev. Letters* **14**, 1022 (1965).
⁵W. C. Koehler, R. M. Moon, A. L. Trego, and A. R. MacKintosh, *Phys. Rev.* **151**, 405 (1966).
⁶Y. Ishikawa, S. Hoshino, and Y. Endoh, *J. Phys. Soc. Japan* **22**, 1221 (1967).
⁷Y. Endoh, Y. Ishikawa, and H. Ohno, *J. Phys. Soc. Japan* **24**, 263 (1968).
⁸A. S. Barker and J. A. Ditzenberger, *Phys. Rev. B* **1**, 4378 (1970).
⁹Y. Hamaguchi, E. O. Wollan, and W. C. Koehler, *Phys. Rev.* **138**, A737 (1965).
¹⁰W. M. Lomer, *Proc. Phys. Soc. (London)* **80**, 489 (1962).
¹¹T. L. Loucks, *Phys. Rev.* **139**, A1181 (1965).
¹²S. Komura, Y. Hamaguchi, and N. Kunitomi, *J. Phys. Soc. Japan* **23**, 171 (1967).
¹³S. Arajs, *J. Appl. Phys.* **39**, 673 (1968).
¹⁴F. Heiniger, *Physik Kondensierten Materie* **5**, 285 (1966).
¹⁵G. T. Meaden, K. V. Rao, and K. T. Tee, *Phys. Rev. Letters* **25**, 359 (1970).
¹⁶N. Mori, Y. Furuya, and T. Mitsui, *J. Phys. Soc. Japan* **28**, 531 (1970).
¹⁷T. Sambongi and T. Mitsui, *J. Phys. Soc. Japan* **24**, 1168 (1968).
¹⁸A. L. Trego and A. R. MacKintosh, *Phys. Rev.* **166**, 495 (1968).
¹⁹T. M. Rice, A. S. Barker, B. I. Halperin, and D. B. McWhan, *J. Appl. Phys.* **40**, 1337 (1969).
²⁰A. Arrott, S. A. Werner, and H. Kendrick, *Phys. Rev.* **153**, 624 (1967).
²¹S. Hoshino, Y. Ishikawa, Y. Yamada, and T. Yamada, *J. Phys. Soc. Japan* **20**, 1729 (1965).
²²M. M. Newmann and K. W. H. Stevens, *Proc. Phys. Soc. (London)* **74**, 290 (1959).
²³N. S. Rajan, R. M. Waterstrat, and P. A. Beck, *J. Appl. Phys.* **31**, 731 (1960).
²⁴K. Schroeder, M. Yessick, and N. P. Baum, *J. Appl. Phys.* **37**, 1019 (1966).
²⁵J. F. Goff (unpublished).
²⁶S. Arajs and G. Dummyre, *J. Appl. Phys.* **37**, 1017 (1966).
²⁷G. DeVries, *J. Phys. Radium* **20**, 438 (1959).
²⁸J. G. Booth, *J. Phys. Chem. Solids* **27**, 1639 (1966).
²⁹Y. Ishikawa, R. Tournier, and J. Filippi, *J. Phys. Chem. Solids* **26**, 1727 (1965).
³⁰Y. Ishikawa, Y. Endoh, H. Hashiura, and H. Ohno, *Solid State Commun.* **4**, 657 (1966).
³¹P. A. Fedders and P. C. Martin, *Phys. Rev.* **143**, 245 (1966).
³²W. Hume-Rothery and G. V. Raynor, *The Structure of Metals and Alloys*, 4th ed. (The Institute of Metals, London, 1962).
³³S. J. Pickart (unpublished).
³⁴C. Herring, *Magnetism* (Academic, New York, 1966), Vol. IV, p. 340.
³⁵A. S. Barker, B. I. Halperin, and T. M. Rice, *Phys. Rev. Letters* **20**, 384 (1968).
³⁶J. Zittartz, *Phys. Rev.* **164**, 575 (1967).
³⁷Y. Hamaguchi and N. Kunitomi, *J. Phys. Soc. Japan* **19**, 1849 (1964).
³⁸A. Giannuzzi, H. Tomaschke, and K. Schroder, *Phil. Mag.* **21**, 479 (1970).
³⁹N. P. Baum and K. Schroder, *Phys. Rev. B* **3**, 3847 (1971).
⁴⁰M. V. Nevitt and A. T. Aldred, *J. Appl. Phys.* **34**, 463 (1963).
⁴¹C. H. Cheng, C. T. Wei, and P. A. Beck, *Phys. Rev.* **120**, 426 (1960).
⁴²D. Bender, *Helv. Phys. Acta* **41**, 400 (1968).
⁴³M. J. Marcinkowski and H. A. Lipsitt, *J. Appl. Phys.* **32**, 1238 (1961).
⁴⁴A. N. Gerritsen, *Handbuch der Physik* (Springer-Verlag, Berlin, 1956), Vol. XIX, p. 137.
⁴⁵B. R. Coles, *Advan. Phys.* **7**, 40 (1958).
⁴⁶P. G. Klemens, *Thermal Conductivity* (Academic, New York, 1969), Vol. I, p. 1.
⁴⁷J. Bardeen, L. N. Cooper, and J. R. Schrieffer, *Phys. Rev.* **108**, 1175 (1957).
⁴⁸J. Bardeen and J. R. Schrieffer, *Progress in Low Temperature Physics* (North-Holland, Amsterdam, 1961), Vol. III, p. 170.
⁴⁹A. H. Wilson, *The Theory of Metals*, 2nd ed. (Cambridge U.P., Cambridge, England, 1954).
⁵⁰M. A. Mitchell and J. F. Goff, *Bull. Am. Phys. Soc.* **16**, 544 (1971).
⁵¹D. B. McWhan and T. M. Rice, *Phys. Rev. Letters* **19**, 846 (1967).